

CLASSIFICATION AND GRADIENT-BASED LOCALIZATION OF CHEST RADIOGRAPHS

Dr. Swapan Das¹, Madhurima Paul², Sutapa Nayak³

¹Assistant Professor, Department Computing & Analytics, NSHM Knowledge Campus, Kolkata, India

²MSc Student, Department Computing & Analytics, NSHM Knowledge Campus, Kolkata, India

³MSc Student, Department Computing & Analytics, NSHM Knowledge Campus, Kolkata, India

Abstract -COVID-19 has infected millions of people worldwide and was declared as a pandemic by the World Health Organization (WHO) on 11th March 2020 considering the extent of its spread throughout the world [59]. Other diseases like viral pneumonia, Lung Opacity (Non-COVID lung infection) affect the lungs leading to severe coughing, fever, and chest pains with similar symptoms of COVID-19. India, being the second-most populous country (136.64 crores) any rapid and low-cost diagnostic tool with high accuracy will be very much required and helpful for both people and healthcare professionals. With this respect Lung disease detected model could be excellent alternatives, cost-effective one because the only input required to be provided to the model is X-ray images. A team of radiologists from New Orleans found that for diagnosing COVID-19 Chest X-rays were faster than reverse-transcription polymerase chain reaction (RT-PCR), especially in areas with limited testing facilities [1]. The radiographs of different viral cases are comparative, and they overlap with other infectious and inflammatory lung diseases, making it hard for radiologists to recognize COVID-19 from other viral cases [2]. Thus this paper presents Lung diseases detected models using deep learning algorithms for automatic detection of diseases like Lung Opacity (Non-COVID lung infection), COVID-19, and Viral Pneumonia from digital chest X-ray images. The project uses the COVID-19 Radiography Database [3] as its dataset. It consists of 21165 Chest X-Ray images belong to 4 different categories such as COVID-19, Lung Opacity, Normal and Viral Pneumonia.

Three top-scoring CNN architectures, VGG-16 [4], ResNet-18 [5], and DenseNet-12 [6], trained on the Image Net Dataset [7], was chosen for fine-tuning on the dataset. The results obtained from the different architectures were then evaluated and compared. Finally, with the help of Gradient weighted Class Activation Maps (Grad-CAM) [8] the affected areas in CXRs were localized.

Key Words: COVID-19, Lung Opacity, Normal and Viral Pneumonia, VGG-16, ResNet-18, DenseNet-121, Deep learning, Grad-CAM

1 INTRODUCTION

Coronavirus disease (COVID-19) is a pandemic disease, which has already caused thousands of casualties and infected several million people worldwide. Any innovative tool which can do quick screening of the COVID-19 disease with high accuracy can be useful to the medical services experts. The main clinical tool currently in use for the diagnosis of COVID-19 is the Reverse transcription-polymerase chain reaction (RT-PCR), which is expensive, less sensitive, uses respiratory specimens for testing [9] and requires specialized medical personnel. RT-PCR, being manual, complicated, laborious, and time-consuming, is used for the detection of COVID-19 patients with a positivity rate of only 63% [9]. Moreover, there is a significant shortage of its supply, which leads to delay in the disease prevention efforts [10]. These delays can lead to infected patients interacting with healthy patients and

infecting them in the process. This is not only an issue for the low-income countries but also certain developed countries are struggling to tackle this [11]. The other diagnosis methods of the COVID-19 include positive pathogenic testing, clinical symptoms analysis, understanding epidemiological history, and positive radiographic images like computed tomography (CT)/Chest radiograph (CXR).

The clinical characteristics of severe COVID-19 infection is that of bronchopneumonia causing fever, cough, dyspnea, and respiratory failure with acute respiratory distress syndrome (ARDS) [12],[13],[14],[15]. The majority of COVID-19 cases have similar features on radiographic images including bilateral, multi-focal, ground-glass opacities with a peripheral or posterior distribution, mainly in the lower lobes [15],[16],[17],[18],[19],[20],[21]. The images of various viral cases of pneumonia, infectious and inflammatory lung diseases overlap with others as they are similar. Therefore, it is difficult for radiologists to distinguish COVID-19 from other lung diseases.

Currently many biomedical health problems and complications (e.g. brain tumor detection, breast cancer detection, etc.) are using Artificial Intelligence (AI) based solutions [22],[23],[24],[25],[26],[27]. Specifically, Convolutional Neural Network (CNN) has been proven extremely beneficial in feature extraction and learning and therefore, widely adopted by the research community [28]. CNN was used to enhance image quality in low-light images from a high-speed video endoscopy [29] and was also applied to identify the nature of pulmonary nodules via CT images, the diagnosis of pediatric pneumonia via chest X-ray images, automated labeling of polyps during colonoscopy videos, cystoscopic image analysis from videos [30],[31],[32],[33]. Vikash et al [34] used the concept of transfer learning in a deep learning framework for the detection of pneumonia with help of pre-trained Image Net models [35] and their ensembles. A VGG-16 model was used by Xianghong et al. [36] for lung region identification and different types of pneumonia classification. For classification and localization of common thoracic diseases, Wang et al [37] used a large hospital-scale dataset and Ronneburger et al [38] used image augmentation on a small

set of images to train deep CNN for image segmentation problems to achieve better performance. Pre-trained DenseNet-121 and feature extraction techniques were used for classification of 14 thoracic diseases using chest radiography [40].

Recently, several groups have reported deep machine learning techniques using X-ray images for detecting COVID-19 pneumonia [42],[43],[44],[45],[46],[47],[48],[49],[50],[51],[52],[53],[54],[55],[56],[57],[58]. However, most of them used a small dataset containing only a few COVID-19 samples. So, it was quite difficult for them to make a generalized model. They cannot guarantee that their performance will remain the same when these models will be tested on a larger dataset. Ioannis et al. [41] used transfer learning technique for a dataset of 1427 X-ray images having 224 COVID-19, 700 Bacterial Pneumonia and 504 Normal X-ray images. The specificity, sensitivity, and accuracy were 96.46%, 98.66%, and 96.78% respectively. They compared different pre-trained models. But they tested on a small dataset. However, Ashfar et al. [45], proposed a Capsule Networks, called COVID-CAPS to deal with a smaller dataset. COVID-CAPS were reported to achieve an accuracy of 95.7%, sensitivity of 90%, and specificity of 95.8%. Abbas et al. [46] have worked on a very small database of 105 COVID-19, 80 Normal, and 11 SARS X-ray images to detect COVID-19 X-ray images using modified pre-trained CNN models to project the high-dimensional feature space into a lower one. This helped to achieve accuracy, sensitivity and specificity of 95.12%, 97.91% and 91.87% respectively. Wang and Wong [42] introduced a deep CNN, called COVID-Net for the detection of COVID-19 cases from around 14k chest X-ray images; however, the achieved accuracy was 83.5%. Ucar et al. [49] used a fine-tuned SqueezeNet pre-trained network with Bayesian optimization to classify COVID-19 images, which showed promising results on a small dataset. Khan et al. [53] used transfer learning technique for classification purposes on a dataset having 327 viral pneumonia, 330 bacterial pneumonia, 310 normal and 284 COVID-19 pneumonia images. Since

different machine learning algorithms were not used in this study, the experimental protocol was not clear in this work.

In summary, several recent works were reported on a small dataset with promising results however these needed to be verified on a large dataset. Some groups have modified or fine-tuned the pre-trained networks to achieve better performance while some groups use capsule networks.

This paper represents techniques for automatic detection and classification of COVID-19, pneumonia and other lung diseases from digital chest X-ray images. The database contains a mixture of 3616 COVID-19, 6012 lung opacity, 1345 viral pneumonia, and 10192 normal chests X-ray images. The high accuracy improves the speed and accuracy of COVID-19 diagnosis of diagnostic tools.

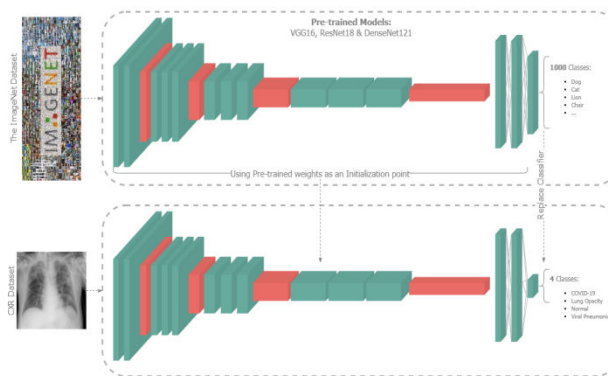
2 METHODOLOGY

2.1 DATABASE DESCRIPTION

A researchers team from Qatar, Qatar University, Doha, and Dhaka University, Bangladesh along with their collaborators from Pakistan and Malaysia have created a chest X-ray images database for COVID-19 positive cases along with Normal, Lung Opacity (Non-COVID lung infection) and Viral Pneumonia images. This project uses the COVID-19 Radiography Database [3]. It has a total of 21165 Chest X-Rays (CXRs) belonging to 4 different classes such as COVID-19, Lung Opacity, Normal and Viral Pneumonia.

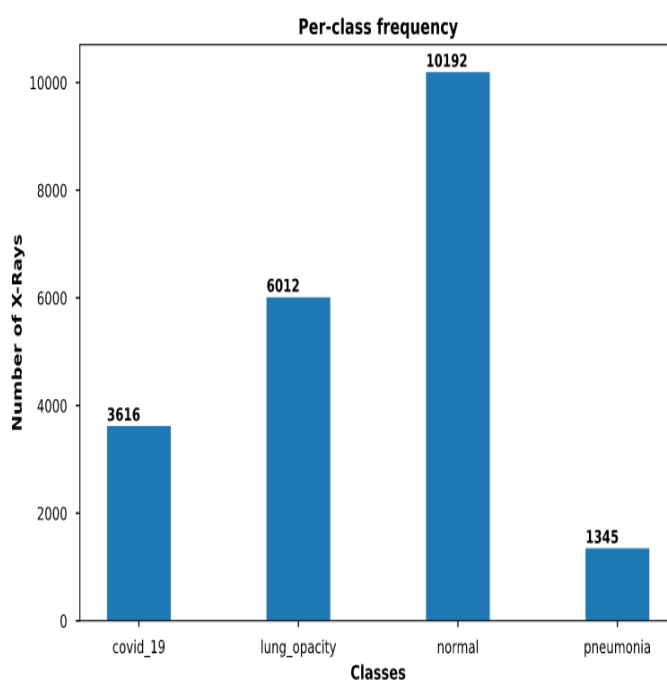
2.2 CNN MODEL SELECTION

Three different pre-trained CNN models were trained, validated and tested in this study. The experimental evaluation of VGG-16[4], DenseNet-121[6] and ResNet18 [5] was performed using PyTorch library with Python running on an Intel © i7-core computer having 3.6GHz processor and 16GB RAM, and also with an 8-GB NVIDIA GeForce GTX 1080 graphics processing unit (GPU) card on 64-bit Windows 10 operating system.



2.3 SPLITTING OF DATASET

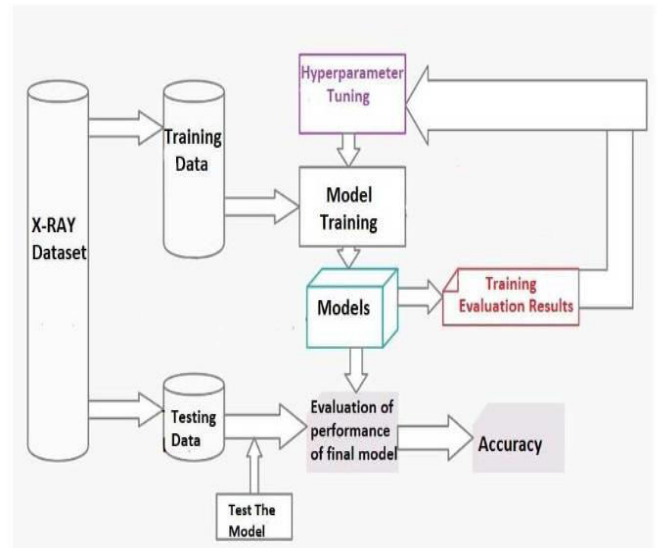
Type	Covid-19	Lung Opacity	Normal	Viral Pneumonia	Total
Train	3496	5892	10072	1225	20685
Val	60	60	60	60	240
Test	60	60	60	60	240



2.4 INVESTIGATION OF THE DEEP LAYER FEATURES

The deep layers feature of the image were investigated by comparing the activated areas of the convolutional layers with the matching regions in the original images. The activation map can take a different range of values and be therefore normalized between 0 and 1. It was observed that the negative activation on dark left/light right edges whereas the strongest channel activates on edges with positive activation on light left/dark right edges.

In the first layer Convolutional neural networks learn to detect features like color and edges. In deeper convolutional layers, the network learns to detect complicated features. By combining features of earlier layers, Convolutional neural networks build up their features. It might be difficult to distinguish COVID-19 and viral pneumonia from the original images as reported by different research groups. However, the deep layer features explain better the reason for a deep learning network's failure or success in a particular decision. It provides a visual explanation of the prediction of CNN and it highlights the regions of the images which are contributing more in classification. This technique will be used in the result to illustrate how this activation mapping distinguishes feature of COVID-19 X-ray images from the other three classes of images i.e. pneumonia, lung opacity and normal X-ray images. The comparative performance for different CNNs for four-class classification is shown in the Result section.



In this study, pre-trained convolutional neural networks have been trained by the dataset of X-Ray images of COVID-19 positive cases along with Normal, Lung Opacity (Non-COVID lung infection) and Viral Pneumonia images. The dataset consists of around 21165 images. Different architectures like, VGG-16, DenseNet-121 and ResNet-18 have been used for experimentation. Reason behind using different models is to compare architectures and to identify which one is best for the application. Fine-tuning of hyperparameters like the number of epochs and the learning rate has also been done to optimize the model complexity and generalize the model.

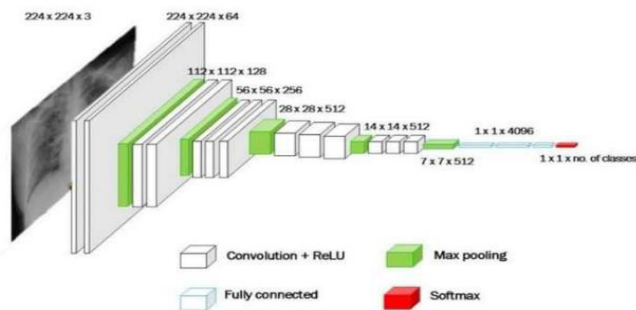
2.6 DEEP LEARNING MODELS

2.6.1 VGG-16

This architecture was found in 2014. The simplicity of this network is the key factor to distinguish it from others. The 3*3 convolutional layers are bundled on top of each other thus increasing the depth of the network. Deduction in volume size is managed by MaxPooling. It also consists of 2 fully connected layers having 4096 nodes each and is followed by a 'Softmax' classifier. This architecture is further classified into 2 types VGG-16 and VGG-19, "16" and "19" represent the number of weight layers in the network. Earlier, both of these networks were considered

2.5 FLOW CHART OF THE METHOD

very deep due to which task of training was quite challenging. To resolve this issue, the creators of the architecture trained smaller versions of VGG with less weight layers. This resulted in the convergence of the smaller networks and was used as ‘Initializers’ for the larger, deeper networks. This process came to be known as pre-training. Even though the process of pre-training is important, it still is a time-consuming and monotonous task since it requires an entire network to be trained beforehand before it can be used as an initializer for the larger network. VGG network has multiple advantages, it can be very good for benchmarking on a particular task. Unfortunately, there are some disadvantages associated with the architecture; it’s training requires lots of time and the weights of network architecture are quite large (in terms of bandwidth). Due to its depth and number of fully-connected nodes, VGG is over 533MB for VGG-16. This makes deploying VGG a tiresome task. Regardless of the disadvantages, VGG architecture is widely used and is considered useful in solving image classification problems.

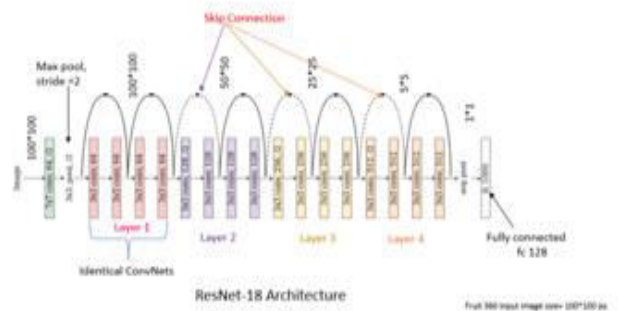


2.6.2 ResNet-18

Deep residual network or ResNet model was developed by He et al. in 2016. This model was formed to defeat problems and difficulties in deep learning training because deep learning training, in general, takes quite a lot of time and is limited to a certain number of layers. The method introduced by ResNet is to apply a skip connection or shortcut. The advantage of the ResNets model compared to other models is that the performance of this model does not decrease even though the architecture is getting deeper.

Here, the computation calculations are made lighter, and the ability to train networks is better. The ResNet model is implemented by skipping connections on two to three layers as shown in the figure having ReLU and batch normalization among the architectures. He et al. showed that the ResNet model performs better in image classification than other models, indicating that the image features were extracted well by ResNet.

If the input data dimensions are identical to the output data dimensions, a residual block on ResNet can be accomplished. In addition, the ResNet-18 ResNet block consists of two layers. The two initial layers of the ResNet architecture resemble GoogleNet by doing convolution 7 × 7 and max-pooling having size 3 × 3 having stride number 2.



networks, DenseNets make use of ‘feature reuse’, which results in elimination of the need to learn redundant feature maps. In DenseNet the number of connections is given by the equation:

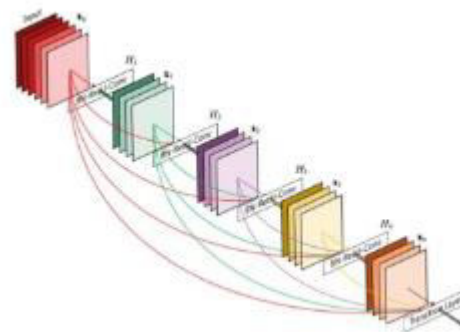
$$\text{Number of connections} = \frac{(L+1)}{2}$$

Logically, in DenseNets, as we would go deeper into the network, there would be a problem of feature map explosion. To counter this problem, the concept of “dense blocks” was introduced. These blocks contain a predefined number of layers within them. Among these layers, the feature maps are shared. The output of a dense block is given to what is known as a ‘transitional layer’, which uses the same concept of bottlenecks, as is used by ResNets, by making 1*1 convolutions followed by MaxPooling to reduce the size of the feature maps

DenseNets propose primarily 2 advantages:

- Parameter Efficiency: Every layer adds only a limited number of parameters, for example in one of the architectures, only 12 kernels were learnt per layer
- Implicit Deep Supervision: Improved flow of gradient through the network, i.e. feature maps in all layers have direct access to the loss function and its gradient.

In this network, each layer in a dense block outputs ‘k’ feature maps, where ‘k’ is the growth rate. A Bottleneck layer consists of 1*1 convolutions followed by 3*3 convolutions; 1*1 convolutions output 4k feature maps. At the output layer, a ‘Softmax’ activation function is used for classification.



Counter-intuitively, even though features are being concatenated in the network with a high number of layers, the model works well as no new filters are involved and the number of filters is predefined by fixing the growth rate. Additionally, despite having a huge number of layers in the network, the number of trainable parameters is only of the order of hundreds of thousands, and was about 0.8 million in one of the architectures, which is approximately 3-4 times less than other networks. This smaller number of trainable parameters has resulted in the prevention of the network being over-fitted.

2.7 GRAD-CAM-APPROACH

Considering previous works, it can be asserted that CNN captures higher-level visual constructs [60], [61]. Moreover, in convolutional features spatial information is naturally retained which is lost in fully connected layers. In the last layers neurons look for semantic class-specific information in the image. To understand the importance of each neuron Grad-CAM uses the gradient information flowing into the last convolutional layer of the CNN. Although our technique is generic enough to visualize any activation in a deep network. To obtain the class discriminative localization map we need to first compute the gradient of the score for class (before the softmax), with respect to feature maps of a convolutional layer. These gradients flowing back are global-average-pooled to obtain the neuron importance. This weight represents a partial linearization of the deep network downstream, and captures the importance of a feature map for a target class. We perform a weighted combination of forward activation maps, and follow it by a ReLU. This

results in a coarse heat-map of the same size as the convolutional feature map. We are only interested in the positive influenced features of class interest. Negative pixels are likely to be part of other categories in the image. As expected, without this ReLU, there are possibilities that localization maps will highlight more than just the desired class and may achieve lower localization performance.

2.8 EXPERIMENT DETAILS

Hyper-parameters

Learning rate	0.00003
Batch Size	32
Number of Epochs	25

Loss Function Categorical Cross-Entropy

Optimizer Adam

Loss Function: Categorical cross entropy is a loss function that is used in multi-class classification tasks. It quantifies the difference between two probability distributions

Optimizer: Adaptive Moment Estimation (adam) is an algorithm used as an optimizer for gradient descent. The method is efficient when working with large problems involving a lot of data or parameters. It requires less memory and is efficient. Intuitively, it is a combination of the ‘gradient descent with momentum’ algorithm and the ‘RMSP(Root Mean Square Propagation)’ algorithm.

2.9 EVALUATION PARAMETER

The efficiency of the model is calculated through various parameters like accuracy, specificity, precision, sensitivity and F1-score. All these parameters can be calculated with the help of a confusion matrix.

Confusion Matrix - A confusion matrix is used to describe the classification model (or “classifier”) performance of a test data set for which the true values are known. True Positives are denoted by ‘TP’ and True Negatives are

denoted by ‘TN’. False Positives and False Negatives are denoted by ‘FP’ and ‘FN’ respectively.

	Class 1 Predicted	Class 2 Predicted
Class 1 Actual	TP	FN
Class 2 Actual	FP	TN

Accuracy –It can be defined as the ratio of correctly predicted observations to the total observations. The model accuracy is calculated by the following formula;

$$\text{Accuracy} = \frac{TP + TN}{TP + TN + FP + FN}$$

Specificity –It can be defined as the ratio of correct negative predictions to the total number of negatives. The specificity of a model is calculated by the following formula

$$\text{Specificity} = \frac{TN}{TN + FP}$$

Precision –It can be defined as the ratio of correctly predicted positive observations to the total predicted positive observations. The Precision of a model is calculated by the following formula

$$\text{Precision} = \frac{TP}{TP + FP}$$

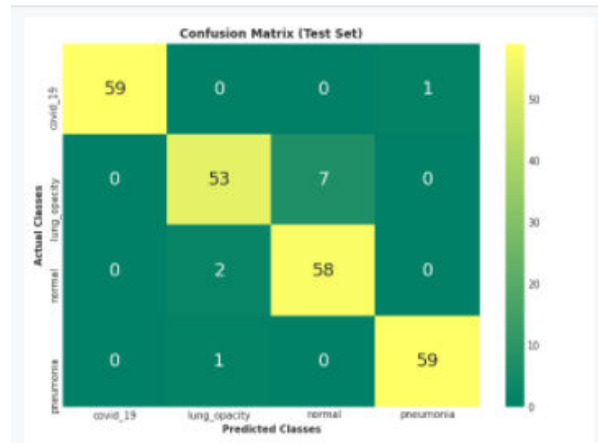
Sensitivity –It is the ratio of correctly predicted positive observations to all observations in actual class. The sensitivity of a model is calculated by the following formula

$$\text{Sensitivity} = \frac{TP}{TP + FN}$$

F1-Score –It can be defined as the weighted average of precision and sensitivity. The F1-score is calculated by the following formula;

$$\text{F1-Score} = \frac{2 * (\text{Sensitivity} * \text{Precision})}{(\text{Sensitivity} + \text{Precision})}$$

2.10 RESULTS, CONFUSION MATRIX, LOSS VS ACCURACY GRAPH AND DISCUSSION

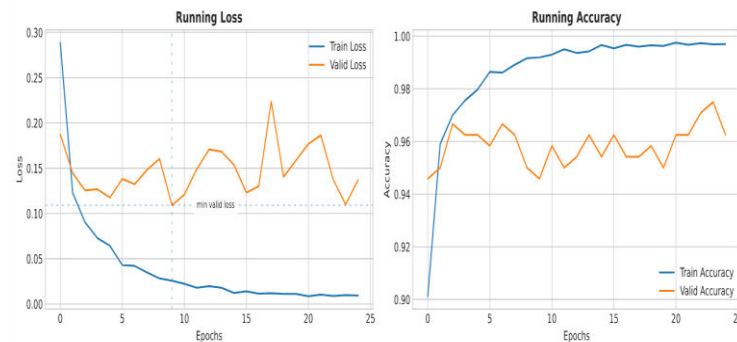
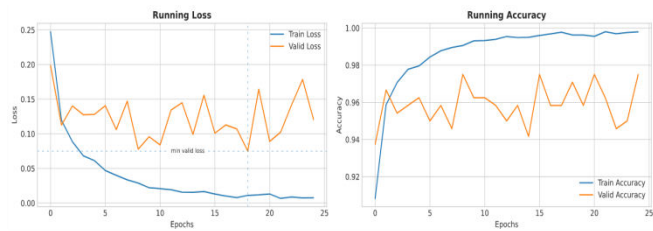
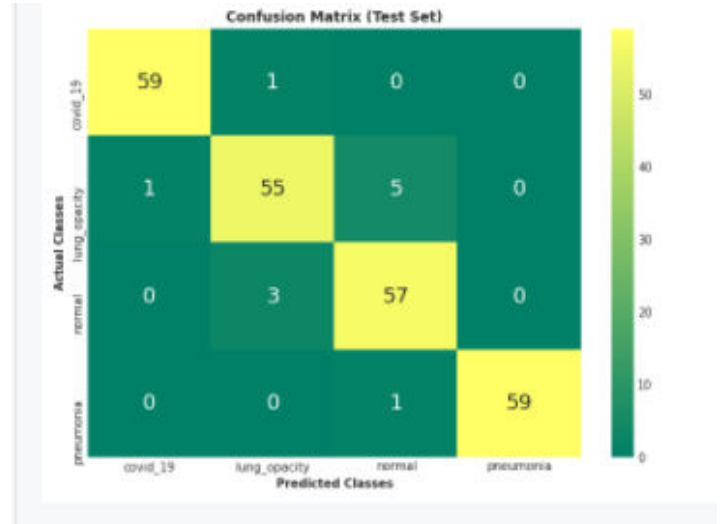
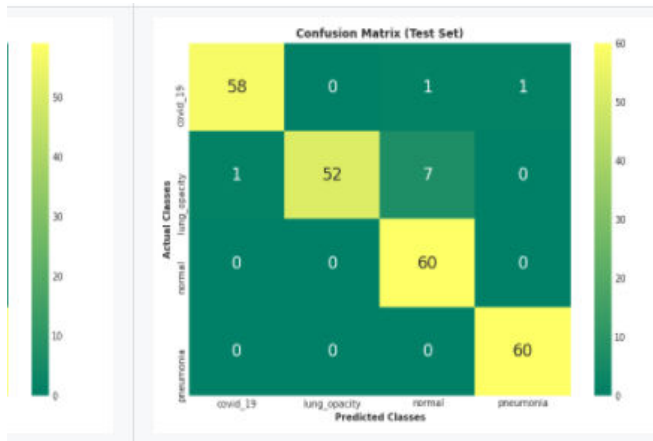


VGG-16 model

VGG-16				
Pathology	Accuracy	Precision	Recall	F1-Score
COVID-19	0.9956	0.9833	1.000	0.9916
Lung Opacity	0.9582	0.8833	0.9464	0.9138
Normal	0.9622	0.9667	0.8923	0.928
Viral Pneumonia	0.9913	0.9833	0.9833	0.9833
TL;DR	Total Correct Predictions		Total Accuracy	
Train set	20362		98.44%	
Test set	229		95.42%	

ResNet-18 model

ResNet-18				
Pathology	Accuracy	Precision	Recall	F1-Score
COVID-19	0.9871	0.9667	0.983	0.9748
Lung Opacity	0.9664	0.8667	1	0.9286
Normal	0.9664	1	0.8823	0.9375
Viral Pneumonia	0.9957	1	0.9836	0.9917
TL;DR	Total Correct Predictions		Total Accuracy	
Train set	20639		99.78%	
Test set	230		95.83%	

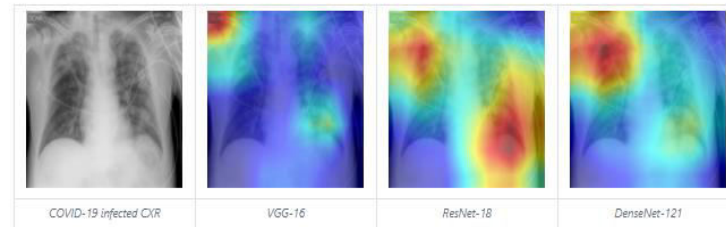


DenseNet-121 model

DenseNet-121				
Pathology	Accuracy	Precision	Recall	F1-Score
COVID-19	0.9957	0.9833	1	0.9916
Lung Opacity	0.9623	0.9167	0.9322	0.9244
Normal	0.9623	0.95	0.9047	0.9268
Viral Pneumonia	0.9957	0.9833	1	0.9916
TL;DR	Total Correct Predictions		Total Accuracy	
Train set	20540		99.30%	
Test set	230		95.83%	

Here we are classifying lung diseases with the help of Gradient-based Class Activation Maps as shown below.

- Localization with Gradient-based Class Activation Maps



3 CONCLUSION

- Having only 7.98 Million parameters DenseNet-121 did relatively better than ResNet-18 and VGG-16 and, with 11.17 Million and 138 Million parameters respectively.
- An increase in the model's parameter count doesn't may achieve better results, but an increase in residual connections might.

- The imbalance data set problem is being resolved by oversampling to a great extent.
- Fine-tuning helped to deal with the comparatively small dataset with respect to the actual data set and speed up the training process.
- GradCAM helps in localizing areas in CXRs which decides a model's predictions.
- The models did a good job distinguishing various lung diseases, which is difficult while doing manually, as mentioned earlier.

REFERENCE

- [1] David L. Smith, John-Paul Grenier, Catherine Batte, and Bradley Spieler. A Characteristic Chest Radiographic Pattern in the Setting of the COVID-19 Pandemic. *Radiology: Cardiothoracic Imaging* 2020 2:5
- [2] Hyun Jung Koo, Soyeoun Lim, JooaeChoe, Sang-Ho Choi, Heungsup Sung, and Kyung-Hyun Do. Radiographic and CT Features of Viral Pneumonia. *RadioGraphics* 2018 38:3, 719-739.
- [3] Tawsifur Rahman, Muhammad Chowdhury, AmithKhandakar. COVID-19 Radiography Database. Kaggle.
- [4] Karen Simonyan, Andrew Zisserman. Very Deep Convolutional Networks for Large-Scale Image Recognition. arxiv:1409.1556v6.
- [5] Kaiming He, Xiangyu Zhang, Shaoqing Ren, Jian Sun. Deep Residual Learning for Image Recognition. arxiv:1512.03385v1.
- [6] Gao Huang, Zhuang Liu, Laurens van der Maaten, Kilian Q. Weinberger. Densely Connected Convolutional Networks. arxiv:1608.06993v5.
- [7] Deng, J. et al., 2009. Imagenet: A large-scale hierarchical image database. In 2009 IEEE conference on computer vision and pattern recognition. pp. 248–255.
- [8] Ramprasaath R. Selvaraju, Michael Cogswell, Abhishek Das, Ramakrishna Vedantam, Devi Parikh, DhruvBatra. Grad-CAM: Visual Explanations from Deep Networks via Gradient-based Localization. arXiv:1610.02391v4
- [9]W. Wang, Y. Xu, R. Gao, R. Lu, K. Han, G. Wu, et al., "Detection of SARS-CoV-2 in different types of clinical specimens", *Jama*, vol. 323, pp. 1843-1844, 2020.
- [10]T. Yang, Y.-C. Wang, C.-F. Shen and C.-M. Cheng, Point-of-Care RNA-Based Diagnostic Device for COVID-19, Basel, Switzerland:Multidisciplinary Digital Publishing Institute, 2020.
- [11]N. Wetsman, Coronavirus Testing Shouldn'T Be This Complicated, 2020, [online] Available: <https://www.theverge.com/2020/3/17/21184015/coronavirus-testing-pcr-diagnostic-point-of-care-cdc-technology>.
- [12]D. Wang, B. Hu, C. Hu, F. Zhu, X. Liu, J. Zhang, et al., "Clinical characteristics of 138 hospitalized patients with 2019 novel Coronavirus—Infected pneumonia in Wuhan China", *JAMA*, vol. 323, no. 11, pp. 1061, Mar. 2020.
- [13]N. Chen, M. Zhou, X. Dong, J. Qu, F. Gong, Y. Han, et al., "Epidemiological and clinical characteristics of 99 cases of 2019 novel coronavirus pneumonia in wuhan China: A descriptive study", *Lancet*, vol. 395, no. 10223, pp. 507-513, Feb. 2020.
- [14]Q. Li, X. Guan, P. Wu, X. Wang, L. Zhou, Y. Tong, et al., "Early transmission dynamics in Wuhan China of novel coronavirus-infected pneumonia", *New England J. Med.*, vol. 382, pp. 1199-1207, Jan. 2020.
- [15]C. Huang et al., "Clinical features of patients infected with 2019 novel coronavirus in Wuhan China", *Lancet*, vol. 395, pp. 497-506, Feb. 2020.
- [16]V. M. Corman et al., "Detection of 2019 novel coronavirus (2019-nCoV) by real-time RT-PCR", *Eurosurveillance*, vol. 25, no. 3, Jan. 2020.
- [17]D. K. W. Chu, Y. Pan, S. M. S. Cheng, K. P. Y. Hui, P. Krishnan, Y. Liu, et al., "Molecular

diagnosis of a novel coronavirus (2019-nCoV) causing an outbreak of pneumonia", *Clin. Chem.*, vol. 66, no. 4, pp. 549-555, Apr. 2020.

- [18]N. Zhang, L. Wang, X. Deng, R. Liang, M. Su, C. He, et al., "Recent advances in the detection of respiratory virus infection in humans", *J. Med. Virology*, vol. 92, no. 4, pp. 408-417, Apr. 2020.
- [19]M. Chung, A. Bernheim, X. Mei, N. Zhang, M. Huang, X. Zeng, et al., "CT imaging features of 2019 novel coronavirus (2019-nCoV)", *Radiology*, vol. 295, no. 1, pp. 202-207, Apr. 2020.
- [20]M. Hosseiny, S. Kooraki, A. Gholamrezanezhad, S. Reddy and L. Myers, "Radiology perspective of coronavirus disease 2019 (COVID-19): Lessons from severe acute respiratory syndrome and middle east respiratory syndrome", *Amer. J. Roentgenology*, vol. 214, no. 5, pp. 1078-1082, May 2020.
- [21]S. Salehi, A. Abedi, S. Balakrishnan and A. Gholamrezanezhad, "Coronavirus disease 2019 (COVID-19): A systematic review of imaging findings in 919 patients", *Amer. J. Roentgenology*, vol. 215, pp. 1-7, Mar. 2020.
- [22]A. M. Tahir, M. E. H. Chowdhury, A. Khandakar, S. Al-Hamouz, M. Abdalla, S. Awadallah, et al., "A systematic approach to the design and characterization of a smart insole for detecting vertical ground reaction force (vGRF) in gait analysis", *Sensors*, vol. 20, no. 4, pp. 957, Feb. 2020.
- [23]M. E. H. Chowdhury, K. Alzoubi, A. Khandakar, R. Khalifa, R. Abouhasera, S. Koubaa, et al., "Wearable real-time heart attack detection and warning system to reduce road accidents", *Sensors*, vol. 19, no. 12, pp. 2780, Jun. 2019.
- [24]M. E. H. Chowdhury, A. Khandakar, K. Alzoubi, S. Mansoor, A. M. Tahir, M. B. I. Reaz, et al., "Real-time smart-digital stethoscope system for heart diseases monitoring", *Sensors*, vol. 19, no. 12, pp. 2781, Jun. 2019.
- [25]K. Kallianos, J. Mongan, S. Antani, T. Henry, A. Taylor, J. Abuya, et al., "How far have we come? Artificial intelligence for chest radiograph interpretation", *Clin. Radiol.*, vol. 74, no. 5, pp. 338-345, May 2019.
- [26]M. Dahmani, M. E. H. Chowdhury, A. Khandakar, T. Rahman, K. Al-Jayyousi, A. Hefny, et al., "An intelligent and low-cost eye-tracking system for motorized wheelchair control", *arXiv:2005.02118*, 2020, [online] Available: <http://arxiv.org/abs/2005.02118>.
- [27]T. Rahman, M. E. H. Chowdhury, A. Khandakar, K. R. Islam, K. F. Islam, Z. B. Mahbub, et al., "Transfer learning with deep convolutional neural network (CNN) for pneumonia detection using chest X-ray", *Appl. Sci.*, vol. 10, no. 9, pp. 3233, May 2020.
- [28]A. Krizhevsky, I. Sutskever and G. E. Hinton, "ImageNet classification with deep convolutional neural networks", *Proc. Adv. Neural Inf. Process. Syst. (NIPS)*, pp. 1097-1105, 2012.
- [29]P. Gómez, M. Semmler, A. Schützenberger, C. Bohr and M. Döllinger, "Low-light image enhancement of high-speed endoscopic videos using a convolutional neural network", *Med. Biol. Eng. Comput.*, vol. 57, no. 7, pp. 1451-1463, Jul. 2019.
- [30]J. Choe, S. M. Lee, K.-H. Do, G. Lee, G. Lee, S. M. Lee, et al., "Deep learning-based image conversion of CT reconstruction kernels improves radiomics reproducibility for pulmonary nodules or masses", *Radiology*, vol. 292, no. 2, pp. 365-373, Aug. 2019.
- [31]D. S. Kermany et al., "Identifying medical diagnoses and treatable diseases by image-based deep learning", *Cell*, vol. 172, no. 5, pp. 1122-1131, 2018.
- [32]M. Negassi, R. Suarez-Ibarrola, S. Hein, A. Miernik and A. Reiterer, "Application of artificial neural networks for automated analysis of cystoscopic images: A review of the current status and future prospects", *World J. Urology*, pp. 1-10, Jan. 2020.

- [33]P. Wang, X. Xiao, J. R. G. Brown, T. M. Berzin, M. Tu, F. Xiong, et al., "Development and validation of a deep-learning algorithm for the detection of polyps during colonoscopy", *Nature Biomed. Eng.*, vol. 2, no. 10, pp. 741-748, Oct. 2018.
- [34]V. Chouhan, S. K. Singh, A. Khamparia, D. Gupta, P. Tiwari, C. Moreira, et al., "A novel transfer learning based approach for pneumonia detection in chest X-ray images", *Appl. Sci.*, vol. 10, no. 2, pp. 559, Jan. 2020.
- [35]D. Gershgorn, *The Data that Transformed AI Research-and Possibly the World*, 2017, [online] Available: <https://qz.com/1034972/the-data-that-changed-the-direction-of-ai-research-and-possibly-the-world/>.
- [36]X. Gu, L. Pan, H. Liang and R. Yang, "Classification of bacterial and viral childhood pneumonia using deep learning in chest radiography", *Proc. 3rd Int. Conf. Multimedia Image Process. ICMIP*, pp. 88-93, 2018.
- [37]X. Wang, Y. Peng, L. Lu, Z. Lu, M. Bagheri and R. Summers, "ChestX-Ray8: Hospital-scale chest X-ray database and benchmarks on Weakly-supervised classification and localization of common thorax diseases", *IEEE CVPR*, pp. 3462-3471, Jul. 2017.
- [38]O. Ronneberger, P. Fischer and T.-N. Brox, "Convolutional networks for biomedical image segmentation", *Int. Conf. Med. Image Comput. Comput.-Assist. Intervent*, 2015.
- [39]P. Rajpurkar et al., "Deep learning for chest radiograph diagnosis: A retrospective comparison of the CheXNeXt algorithm to practicing radiologists", *PLOS Med.*, vol. 15, no. 11, Nov. 2018.
- [40]T. K. Ho and J. Gwak, "Multiple feature integration for classification of thoracic disease in chest radiography", *Appl. Sci.*, vol. 9, no. 19, pp. 4130, Oct. 2019.
- [41]P. Lakhani and B. Sundaram, "Deep learning at chest radiography: Automated classification of pulmonary tuberculosis by using convolutional neural networks", *Radiology*, vol. 284, no. 2, pp. 574-582, Aug. 2017.
- [42]L. Wang and A. Wong, "COVID-Net: A tailored deep convolutional neural network design for detection of COVID-19 cases from chest X-ray images", *arXiv:2003.09871*, 2020, [online] Available: <http://arxiv.org/abs/2003.09871>
- [43]S. Wang et al., "A deep learning algorithm using CT images to screen for corona virus disease (COVID-19)", *medRxiv*, vol. 24, pp. 2020.02, Apr. 2020.
- [44]A. S. Joaquin, *Using Deep Learning to Detect Pneumonia Caused by NCOV-19 From X-Ray Images*, 2020, [online] Available: <https://towardsdatascience.com/using-deep-learning-to-detect-ncov-19-from-x-ray-images-1a89701d1acd>
- [45]I. D. Apostolopoulos and T. A. Mpesiana, "Covid-19: Automatic detection from X-ray images utilizing transfer learning with convolutional neural networks", *Phys. Eng. Sci. Med.*, vol. 43, no. 2, pp. 635-640, Jun. 2020.
- [46]A. Abbas, M. M. Abdelsamea and M. M. Gaber, "Classification of COVID-19 in chest X-ray images using DeTraC deep convolutional neural network", *arXiv:2003.13815*, 2020, [online] Available: <http://arxiv.org/abs/2003.13815>.
- [47]E. E.-D. Hemdan, M. A. Shouman and M. E. Karar, "COVIDX-Net: A framework of deep learning classifiers to diagnose COVID-19 in X-ray images", *arXiv:2003.11055*, 2020, [online] Available: <http://arxiv.org/abs/2003.11055>.
- [48]A. Narin, C. Kaya and Z. Pamuk, "Automatic detection of coronavirus disease (COVID-19) using X-ray images and deep convolutional neural networks", *arXiv:2003.10849*, 2020, [online] Available: <http://arxiv.org/abs/2003.10849>.
- [49]J. Zhang, Y. Xie, Z. Liao, G. Pang, J. Verjans, W. Li, et al., "Viral pneumonia screening on chest X-ray images using confidence-aware anomaly

- detection", *arXiv:2003.12338*, 2020, [online] Available: <http://arxiv.org/abs/2003.12338>.
- [50]P. K. Sethy and S. K. Behera, "Detection of coronavirus disease (covid-19) based on deep features", *Preprints*, 2020.
 - [51]P. Afshar, S. Heidarian, F. Naderkhani, A. Oikonomou, K. N. Plataniotis and A. Mohammadi, "COVID-CAPS: A capsule network-based framework for identification of COVID-19 cases from X-ray images", *arXiv:2004.02696*, 2020, [online] Available: <http://arxiv.org/abs/2004.02696>.
 - [52]T. Ozturk, M. Talo, E. A. Yildirim, U. B. Baloglu, O. Yildirim and U. Rajendra Acharya, "Automated detection of COVID-19 cases using deep neural networks with X-ray images", *Comput. Biol. Med.*, vol. 121, Jun. 2020.
 - [53]F. Ucar and D. Korkmaz, "COVIDagnosis-Net: Deep Bayes-squeezenet based diagnosis of the coronavirus disease 2019 (COVID-19) from X-ray images", *Med. Hypotheses*, vol. 140, Jul. 2020.
 - [54]L. O. Hall, R. Paul, D. B. Goldgof and G. M. Goldgof, "Finding covid-19 from chest X-rays using deep learning on a small dataset", *arXiv:2004.02060*, 2020, [online] Available: <https://arxiv.org/abs/2004.02060>.
 - [55]H. S. Maghdid, A. T. Asaad, K. Z. Ghafoor, A. S. Sadiq and M. K. Khan, "Diagnosing COVID-19 pneumonia from X-ray and CT images using deep learning and transfer learning algorithms", *arXiv:2004.00038*, 2020, [online] Available: <http://arxiv.org/abs/2004.00038>.
 - [56]S. Minaee, R. Kafieh, M. Sonka, S. Yazdani and G. JamalipourSoufi, "Deep-COVID: Predicting COVID-19 from chest X-ray images using deep transfer learning", *arXiv:2004.09363*, 2020, [online] Available: <http://arxiv.org/abs/2004.09363>.
 - [57]X. Li, C. Li and D. Zhu, "COVID-MobileXpert: On-device COVID-19 screening using snapshots of chest X-ray", *arXiv:2004.03042*, 2020, [online] Available: <http://arxiv.org/abs/2004.03042>.
 - [58]A. I. Khan, J. L. Shah and M. M. Bhat, "CoroNet: A deep neural network for detection and diagnosis of COVID-19 from chest X-ray images", *Comput. Methods Programs Biomed.*, vol. 196, Nov. 2020
 - [59]WHO Director-General's Opening Remarks at the Media Briefing on COVID-19—11 March 2020, 2020, [online] Available: <https://www.who.int/dg/speeches/detail/who-director-general-s-opening-remarks-at-the-media-briefing-on-covid-19-11-march-2020>.
 - [60]Y. Bengio, A. Courville, and P. Vincent. Representation learning: A review and new perspectives. *IEEE transactions on pattern analysis and machine intelligence*, 35(8):1798–1828, 2013
 - [61] A. Mahendran and A. Vedaldi. Visualizing deep convolutional neural networks using natural pre-images. *International Journal of Computer Vision*, pages 1–23, 2016

Authors Email address:

1. Dr. Swapan Das(swapan.d11@gmail.com)
2. Madhurima Paul (mguharoy4@gmail.com)
3. SutapaNayak (rtsutapa800@gmail.com)